Porphyrin and Fullerene Covalently Functionalized Graphene Hybrid Materials with Large Nonlinear Optical Properties

Zhi-Bo Liu,[†] Yan-Fei Xu,[‡] Xiao-Yan Zhang,[‡] Xiao-Liang Zhang,[†] Yong-Sheng Chen,*,[‡] and Jian-Guo Tian*,[†]

The Key Laboratory of Weak Light Nonlinear Photonics, Ministry of Education, Teda Applied Physics School, Nankai University, Tianjin 300457, P.R. China, and Key Laboratory for Functional Polymer Materials and Centre for Nanoscale Science and Technology, Nankai University, Tianjin 300071, P.R. China

The nonlinear optical properties of two novel graphene nanohybrid materials covalently functionalized with porphyrin and fullerene were investigated by using the Z-scan technique at 532 nm in the nanosecond and picosecond time scale. Results show that covalently functionalizing graphene with the reverse saturable absorption chromospheres porphyrin and fullerene can enhance the nonlinear optical performance in the nanosecond regime. The covalently linked graphene nanohybrids offer performance superior to that of the individual graphene, porphyrin, and fullerene by combination of a nonlinear mechanism and the photoinduced electron or energy transfer between porphyrin or fullerene moiety and graphene.

Introduction

Materials with large third-order optical nonlinearities and fast nonlinear optical (NLO) response are usually considered to be promising candidates for photonic applications such as optical communication, optical limiting, optical data storage, information processing, and so on. The major requirements of such materials, in addition to large NLO response, are low losses at the wavelength of interest, good optical quality, and mechanical stability, together with easy preparation procedures and low cost. Extensive research has been conducted in the past 20 years and led to the emergence of three main classes of nonlinear optical materials: reverse saturable absorbers, multiphoton absorbers, and nonlinear scattering systems.[1–3] However, none of these systems, taken individually, is able to fully fulfill the requirements listed above. Some attempts were first performed with combinations of NLO materials in cascaded geometries: multiplate or tandem cells.[4] Then, a physically blended system of two kinds of NLO materials was used to enhance nonlinear transmittance by complementary nonlinear mechanisms, such as reverse saturable absorption (RSA) dye blended with single-walled carbon nanotubes (SWNT).[5–7] Recently, covalently linked porphyrin-carbon nanotube structure presented NLO properties larger than those of the blended samples and individual components as a result of the charge-separated excited state produced by photoinduced electron transfer from the electron-donating porphyrin moiety to the electron-accepting SWNTs.[8,9] Hence, covalent or noncovalent combinations of NLO materials may be a better approach to improve NLO properties of materials than the modification of individual nonlinear optical material. However, reports on optical nonlinearities of combination systems are few as yet, especially for covalently combined materials.

Among large numbers of NLO materials, porphyrins[10,11] and fullerenes[12,13] with large π-conjugated structures have been extensively investigated and exhibit strong nonlinear absorption (NLA) due to their higher excited-state absorption cross sections compared with ground-state absorption cross sections. Allotropic carbon nanomaterials of fullerenes, carbon nanotubes, and grapheme all have also unique electrical, optical, and mechanical properties. Especially for graphene, it has been a very recent rising star in material science with atomically thin.[14–16] We have observed large NLO properties in graphene oxide (GO)[17] and strong optical limiting effects in graphene-porphyrin hybrid material.[18] Therefore, we expect that combining the two-dimensional (2D) nanoscale graphene with optoelectronically active porphyrin and fullerene molecules would feature not only the intrinsic properties of graphene, porphyrin, and fullerene but also in some circumstances new behaviors and functions arising from the mutual π interaction between graphene and porphyrin or fullerene, and an enhanced NLO behavior compared with that of the individual graphene, porphyrin, and fullerene may be generated. In this paper, we report the nonlinear optical properties of two novel graphene hybrid materials covalently functionalized with porphyrin and fullerene at 532 nm. In the meantime, the mechanism for the NLO responses of these two graphene hybrid materials is discussed.

Experimental Section

The synthesis of a porphyrin-graphene nanohybrid, Graphene-TPP (Scheme 1), was carried out using an amine-functionalized prophyrin (TPP-NH$_2$) and graphene oxide in DMF. For the fullerene-graphene nanohybrid, Graphene-C$_{60}$ (Scheme 2), pyrrolidine fullerene (C$_{60}$(OH)$_x$), and graphene oxide in DMF were used for the synthesis via a mild coupling reaction between the −OH group of pyrrolidine fullerene and the −COOH group of GO.[19] Large scale and water-soluble graphene oxide was prepared by a modified Hummers method.[20] DMF was purified under vacuum. Results of atomic force microscopy (AFM), thermogravimetry analysis (TGA), and X-ray diffraction (XRD) characterization have confirmed that this graphene material can be easily dispersed at the state of complete exfoliation consisting of almost entire single-layered graphene sheets in H$_2$O.[20] TPP-NH$_2$ and graphene oxide molecules are covalently bonded

* To whom correspondence should be addressed. E-mail: jjtian@nankai.edu.cn, yschen99@nankai.edu.cn.
† The Key Laboratory of Weak Light Nonlinear Photonics.
‡ Key Laboratory for Functional Polymer Materials and Centre for Nanoscale Science and Technology.

SCHEME 1: Synthesis Schema of Graphene-TPP
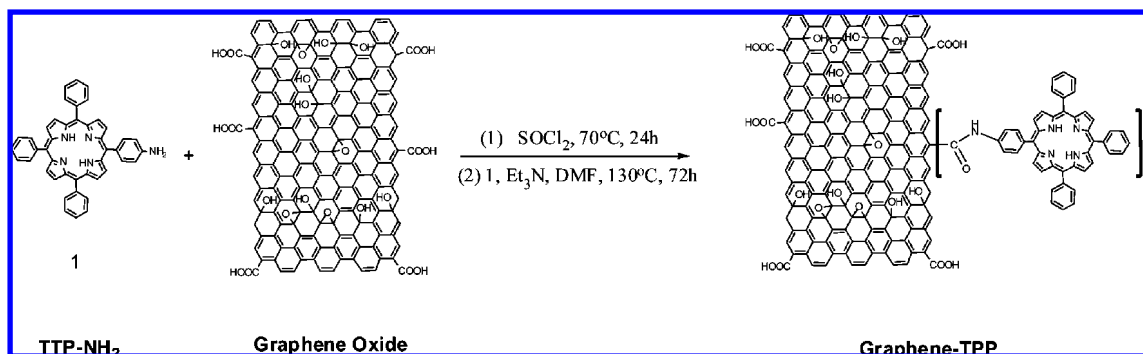
SCHEME 2: Synthesis Schema of Graphene-C$_{60}$
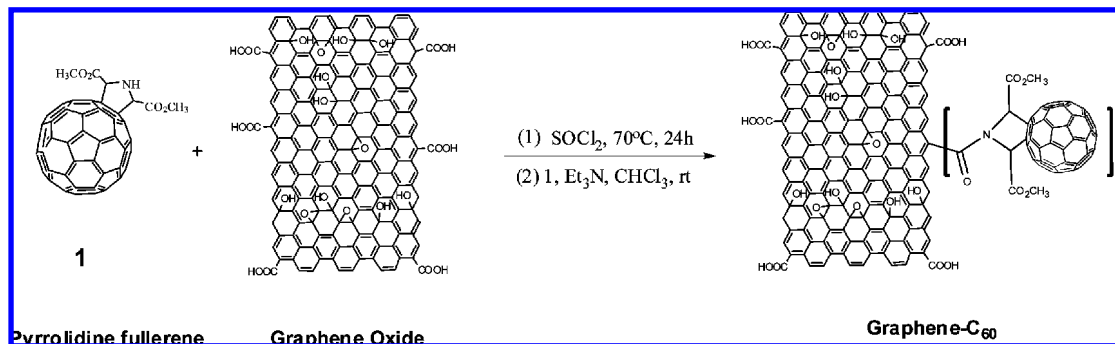
together with an amide bond. Much care has been taken to make sure that all unreacted TPP-NH$_2$ has been removed using extensive solvent washing, sonication, and membrane filtration. The attachment of organic molecules to graphene oxide has made Graphene-TPP soluble in DMF and other polar solvents. For Graphene-C$_{60}$, a large excess of pyrrolidine fullerene was used for the reaction, and the unreacted fraction was removed by cycles of centrifugation and washing. On the basis of UV and elemental analysis measurements, it was estimated that one C$_{60}$ was roughly covalently attached for 104 carbon atoms in graphene and one porphyrin was attached for 874 carbon atoms. The average C$_{60}$−C$_{60}$ distance is about 3 nm, and the average TPP−TPP distance is about 23 nm.

The nonlinear optical properties of these materials were measured by Z-scan technique in the nanosecond and picosecond regimes. The Z-scan experiments are preformed with linearly polarized 5-ns and 35-ps pulses at 532 nm generated from a frequency doubled Q-switched Nd:YAG laser and a mode-locked Nd:YAG laser (Continuum model PY61), respectively. The spatial profiles of the pulses are of nearly Gaussian form after spatial filtering. The pulses are split into two parts: the reflected pulses were used as reference, and the transmitted pulses were focused onto samples by using a 25-cm focal length lens. The sample was placed at the focus where the spot radius of pulses was about 20 μm. The reflected and transmitted pulses energies were measured simultaneously with two energy detectors (Molectron J3S-10). C$_{60}$ was employed as a standard. In the measurements, all of the sample concentrations were adjusted to have the same linear transmittance of 75% at 532 nm in 1-mm-thick cells.

A experimental setup similar to that for the Z-scan experiments was used to measure the nonlinear scattering signal. The transmitted pulses were focused onto samples by using a 25-cm focal length lens (L1). The sample was placed at the focus where the spot radius of the pulses was about 20 μm. After traveling the nonlinear samples, the beam was attenuated and imaged on a CCD camera (Spiricon USB L230) through a 25-cm focal length lens (L2). L2 with a diameter of 5 cm was placed 5-cm after the beam focus. In the measurements of nonlinear scattering signals, a baffle with 3-mm diameter was attached to lens L2 to remove the impact of the input laser beam in order to observe better scattering signals.

Results and Discussion

Linear Absorption Spectra. Figure 1 gives UV−vis absorption spectra of Graphene-TPP, TPP-NH$_2$, Graphene-C$_{60}$, pyrrolidine fullerene, and GO in DMF. Graphene oxide shows a strong absorption band at 268 nm. The TPP-NH$_2$ spectrum exhibits a strong Soret absorption at 419 nm and weak Q-bands between 500 and 700 nm, which is consistent with that of TPP-NH$_2$ analogues.[24] A similar band is also observed for Graphene-TPP and the controlled sample of graphene oxide with TPP-NH$_2$ in DMF (1:1 w/w) at 419 nm corresponding to the Soret band of TPP moiety, and no obvious shift is observed. The hybrid Graphene-TPP exhibits a broad absorption at 280 nm, which should be the corresponding graphene oxide peak at 268 nm with a red shift of 12 nm. The controlled sample exhibits a broad absorption band at 274 nm with a red shift of 6 nm. These results indicate that at ground state the attachment of TPP moiety had made some perturbations in the electronic state of GO, but no observable change can be seen for the TPP part. The hybrid Graphene-C$_{60}$ exhibits a similar band to GO and pyrrolidine fullerene (as shown in Figure 1b). The results for concentration dependence of the UV−vis absorption show that there is no aggregation and Graphene-TPP hybrid was homogeneously dispersed in DMF.[18]

After photoexcitation, the intramolecular donor−acceptor interaction between the two moieties of TPP-NH2 and graphene in our Graphene-TPP nanohybrid may include a charge transfer from the photoexcited singlet TPP-NH$_2$ to the graphene moiety, which results in the observed fluorescence quenching and energy

Functionalized Graphene Hybrid Materials

J. Phys. Chem. B, Vol. 113, No. 29, 2009 **9683**
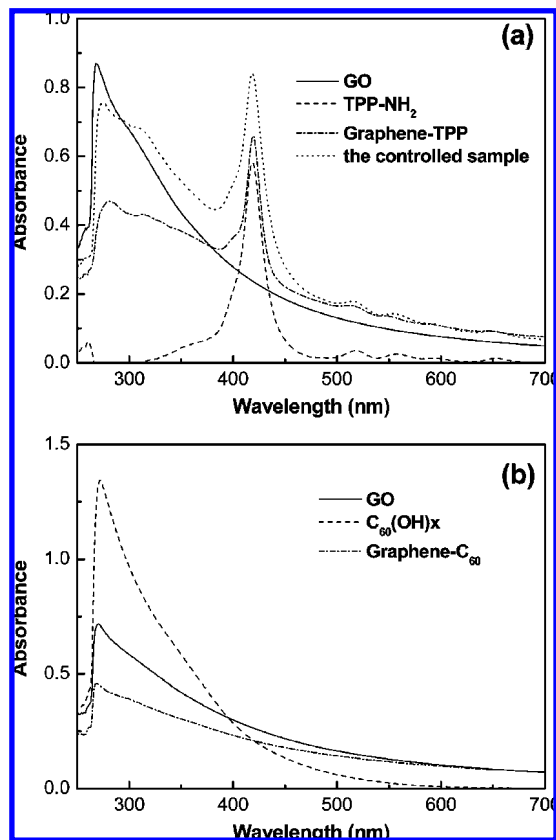
Figure 1. UV−vis absorption spectra of Graphene-TPP, TPP-NH$_2$, the controlled sample, Graphene-C$_{60}$, pyrrolidine fullerene, and GO in DMF.

Figure 2. (a) FTIR spectra of TPP-NHCO-SPFGraphene, TPP-NH$_2$, and graphene oxide. (b) FTIR spectra of GO, pyrrolidine fullerene, and graphene-C60.

release.[18] In this Graphene-TPP, the effective intramolecular quenching may be explained by the extended conjugated π-system of graphene and the porphyrin mediated by a through-bond mechanism, due to the unique direct linkage mode of the two moieties by the amide bond.[9]

Fourier Transform Infrared Spectroscopy. Figure 2a shows Fourier transform infrared spectroscopy (FTIR) spectra of Graphene-TPP, TTP-NH$_2$, and GO. In the spectrum of graphene oxide, the peak at 1730 cm^{-1} was the characteristic C=O stretch of the carboxylic group on the GO. In the spectrum of Graphene-TPP, the peak at 1730 cm^{-1} almost disappeared and a new broadband emerged at 1640 cm^{-1} corresponding to the C=O characteristic stretching band of the amide group.[10] The stretching band of amide C−N peak appeared at 1260 cm^{-1}. These results clearly indicated that the TTP-NH$_2$ molecules had been covalently bonded to the GO via the amide linkage. Figure 2b shows the FTIR spectra of GO, pyrrolidine-C$_{60}$, and the Graphene-C$_{60}$ hybrid. As shown in Figure 2b, the notable FTIR feature of GO is the absorption band corresponding to the carboxyl stretching at 1730 cm^{-1}. The peak at 1630 cm^{-1} is attributed to the deformation of the O−H band of the strongly intercalated water absorbed by GO. The peak at 1746 cm^{-1} in the pyrrolidine-C$_{60}$ is the vibration of the -COOCH$_3$ group. The Graphene-C$_{60}$ hybrid has two main peaks at 1725 and 1636 cm^{-1}. The broad peak at 1725 cm^{-1} may be attributed to the overlapping of the remaining carboxyl group in the graphene and the ester group in the pyrrolidine-C$_{60}$. Also, there is a new peak at 1636 cm^{-1} in the Graphene-C$_{60}$ hybrid, which can be assigned to the amide carbonyl stretching mode. This indicates that C$_{60}$ is chemically attached to the graphene sheet.

Nonlinear Optical Properties. The nonlinear optical properties of these materials were measured by Z-scan technique[21] in
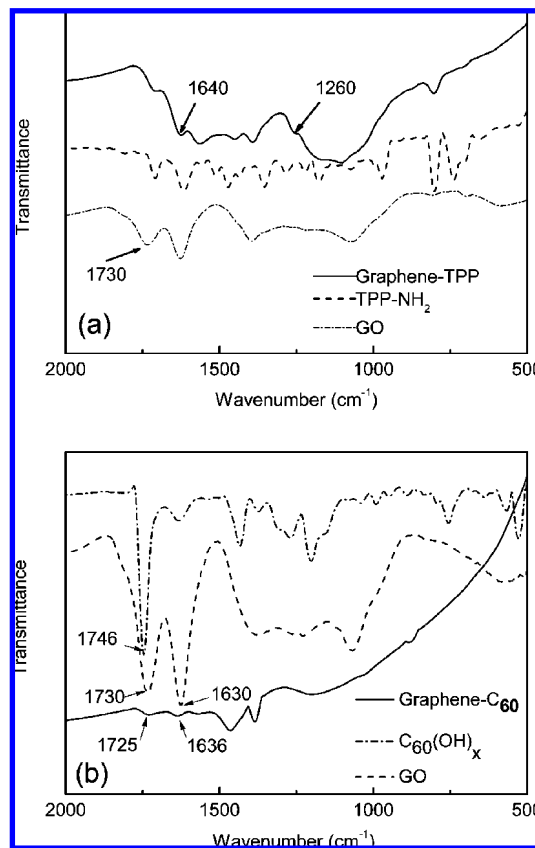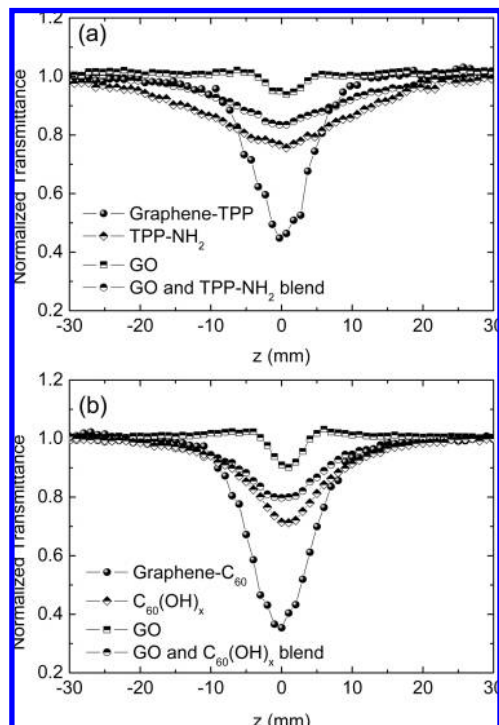
the nanosecond and picosecond regime. Figure 3a shows open-aperture Z-scan results of Graphene-TPP, TPP-NH$_2$, graphene oxide, and a controlled blend sample of TPP-NH$_2$ with graphene oxide (1:1 w/w) at 532 nm with 5-ns pulses. The open aperture Z-scan measures the transmittance of the sample as it translates through the focal plane of a tightly focused beam. As the sample is brought closer to focus, the beam intensity increases and the nonlinear effect increases, which leads to a decreasing transmittance for reverse saturable absorption (RSA), two-photon absorption (TPA), and nonlinear scattering. As shown in Figure 3a, the Graphene-TPP has the largest dip among the transmittance curves of the studied materials (Graphene-TPP, TPP-NH$_2$, graphene oxide, and the controlled sample). At the focal point where the input fluence is maximum, the transmittances of Graphene-TPP, TPP-NH$_2$, graphene oxide, and the controlled sample drop down to 44.8%, 75.6%, 93.8%, and 83.5%, respectively. Therefore, Graphene-TPP demonstrated much better nonlinear optical properties compared with those of the controlled sample and the individual components (TTP-NH$_2$ and graphene oxide) of the hybrid.

Under the same experimental conditions, we also carried out the nanosecond open-aperture Z-scan experiments to study the NLO performance of GO, Graphene-C$_{60}$, GO/pyrrolidine fullerene blend, and pyrrolidine fullerene, as shown in Figure 3b. At focal point, the transmittances of Graphene-C$_{60}$, pyrrolidine fullerene, graphene oxide, and GO/ pyrrolidine fullerene blend drop down to 35.4%, 71.3%, 90.1%, and 79.8%, respectively. These results demonstrate that although excellent nonlinear optical properties were observed for all of the samples, the largest dip for the Graphene-C$_{60}$ hybrid among the transmittance curves indicates that it is the best one.[8] In the meantime, compared with Z-scan
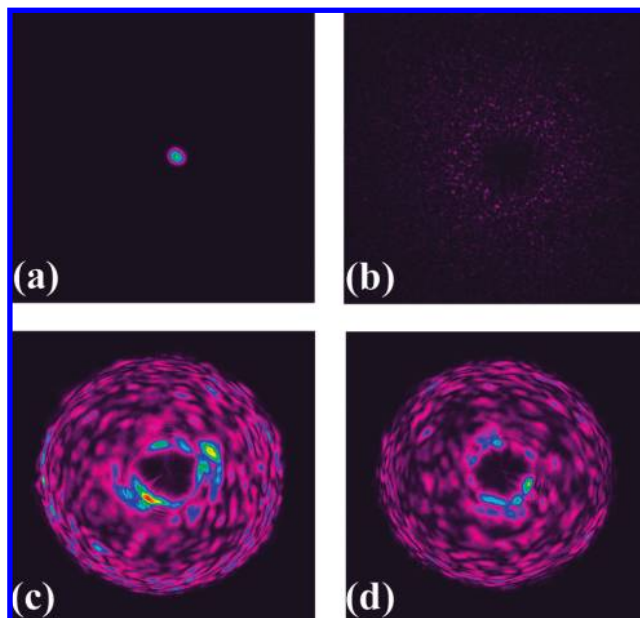
Figure 3. (a) Open-aperture Z-scan curves of Graphene-TPP, TPP-NH$_2$, graphene oxide, and a controlled blend sample of TPP-NH$_2$ with graphene oxide (1:1 w/w). (b) Open-aperture Z-scan curves of Graphene-C$_{60}$, pyrrolidine fullerene, graphene oxide, and a controlled blend sample of pyrrolidine fullerene with graphene oxide (1:1 w/w) at 532 nm with 5-ns pulses.
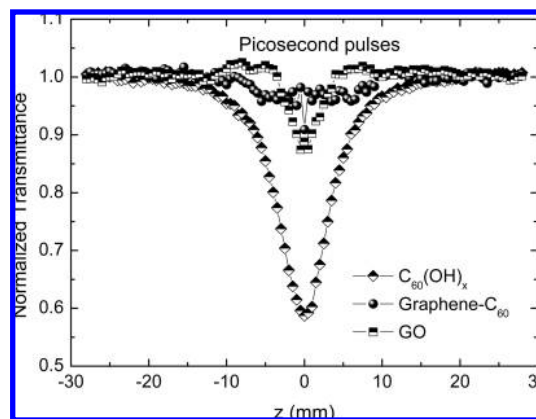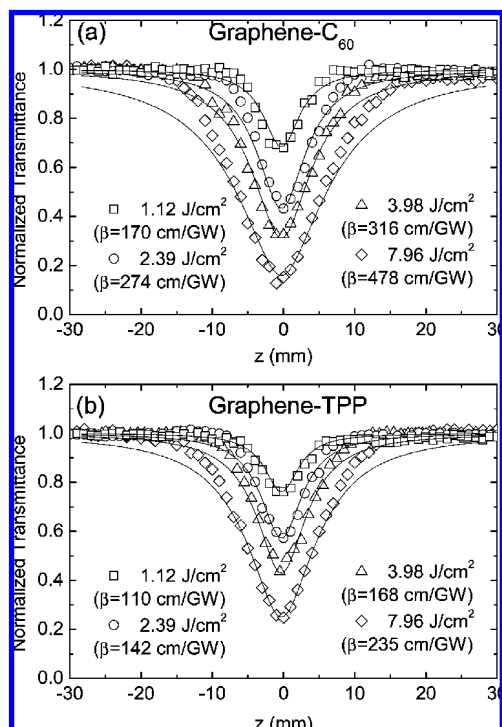

Figure 4. Images of input laser beam (a) and scattering light (b, c, d) when the samples Graphene-C$_{60}$ and Graphene-TPP were fixed on the focus. (b) Input fluence was low and weak nonlinear scattering signal was observed. (c, d) Strong nonlinear scattering signals for Graphene-C$_{60}$ and Graphene-TPP.

Figure 5. Open-aperture Z-scan curves of Graphene-C$_{60}$, pyrrolidine fullerene, and GO with picosecond pulses.

results of Graphene-TPP shown in Figure 3a, the larger dip of Z-scan curves of Graphene-C$_{60}$ indicates that it exhibits better nonlinear optical response than Graphene-TPP. From Figure 3, we can obviously see that both Graphene-TPP and Graphene-C$_{60}$ have NLO properties larger than those of the blended samples and their two parents. Therefore, the graphene hybrid materials covalently functionalized with porphyrin and fullerene are better candidates for applications in optical limiting than the individual graphene, porphyrin, or fullerene.

Different mechanisms exist for NLO, such as nonlinear absorption (multiphoton absorption, reverse saturable absorption (RSA)), nonlinear refraction (electronic or thermal effects), and nonlinear light scattering.[1] Closed-aperture Z-scan experiments have also been carried out to measure their nonlinear refraction, and the results showed that no obvious nonlinear refraction was observed in Graphene-TPP or Graphene-C$_{60}$. The NLO properties of fullerene and porphyrin come from the conjugative effect of molecules, according to reverse saturable absorption mechanism, i.e., their first singlet and triplet states have larger absorption cross sections than the ground state. For GO, we studied its NLO properties and found that two-photon absorption is the dominating nonlinear absorption mechanism in the picosecond regime and a large excited state absorption in the nanosecond regime.[17] In addition, carbon nanotubes (CNTs), another allotropic carbon nanostructure, have also been reported to have strong optical limiting effects, which arise from strong nonlinear light scatterings due to the creation of new scattering centers consisting of ionized carbon microplasmas and solvent microbubbles.[22−24]

The reason that Graphene-C$_{60}$ and Graphene-TPP hybrids exhibit the good NLO performance is not yet understood. However, from the similar electronic structures of C$_{60}$, graphene, and CNTs, it is reasonable to expect that both a nonlinear absorption and a nonlinear light scattering mechanism may play a role in the hybrid's enhanced NLO performance. Actually, during the measuring process, both Graphene-C$_{60}$ and Graphene-TPP exhibited obvious nonlinear scattering signals. Figure 4 gives the images of input laser beam (a) and scattering light (b, c, d) when Graphene-C$_{60}$ and Graphene-TPP were fixed on the focus. The details of the measurements of the images are described in the Experimental Section. In order to observe the scattering signal better, a 3-mm diameter baffle was used to remove the impact of the input laser beam. When the input fluence was low (<0.1 J/cm^2), no obvious scattering signal was observed, as shown in Figure 4b. When a large input fluence (7.96 J/cm^2) was used, strong nonlinear scattering signals were observed for Graphene-C$_{60}$ (Figure 4c) and Graphene-TPP (Figure 4d), which may be assigned to the fast growth of hot carbon vapor bubbles resulting from the incandescence and submission of graphitic particles, as the mechanism of CNTs.[22−24]

Figure 5 shows the open-aperture Z-scan results of Graphene-C$_{60}$, pyrrolidine fullerene, and GO at 532 nm with 35-ps pulses. Unlike in the nanosecond regime, Graphene-C$_{60}$ exhibits a very weak NLO property in the picosecond regime. The NLO

Functionalized Graphene Hybrid Materials

J. Phys. Chem. B, Vol. 113, No. 29, 2009 **9685**

Figure 6. Open-aperture Z-scan curves of Graphene-C_{60} (a) and Graphene-TPP (b) with different input fluence at 532 nm in the nanosecond regime.

scattering performance in the nanosecond regime, which is different from the individual components of GO, porphyrin, and fullerene. Furthermore, another possible reason for this enhanced NLO performance may be attributed to the possible photoinduced electron and/or energy transfer mechanism between graphene and fullerene or porphyrin. In the graphene-TPP system, porphyrin is a favorable electron donor and graphene is an electron acceptor when the two moieties are connected directly. Therefore, as in the CNT-porphyrin system,[25] the intramolecular donor−acceptor interaction between the two moieties of TPP and graphene in our Graphene-TPP nanohybrid may have a charge transfer from the photoexcited singlet TPP to graphene moiety, and this results in the fluorescence quenching and energy releasing.[18] Similarly, photoinduced electron transfer between graphene and fullerene (like the carbon nanotubes-C_{60} system[26]) has been also observed in the Graphene-C_{60} system.[19] It is known that the photoinduced electron transfer can result in an enhanced NLO performance, as observed in the PVK-modified SWCNTs system[27] and the SWNT-porphyrin system.[8] Therefore, the greatly enhanced NLO performance of Graphene-C_{60} and Graphene-TPP should arise from a combination of photoinduced electron and/or energy transfer, RSA, TPA, and nonlinear scattering mechanisms. Similar results have been observed in hybrid materials of carbon nanotubes with porphyrins.[8,9]

Conclusions

In summary, we have reported the NLO properties of two graphene hybrid materials. Results show that covalently functionalizing graphene with RSA chromospheres porphyrin and fullerene can enhance the NLO performance in the nanosecond regime. The covalently linked graphene nanohybrids offer performance superior to that of the individual GO, porphyrin, and fullerene by combination of a nonlinear mechanism and the photoinduced electron or energy transfer between porphyrin or fullerene moiety and graphene. With the abundant and highly pure functionalized graphene materials readily available, unique structure, and excellent NLO properties, we expect reasonedly that these processable functionalized graphene materials can bring a competitive entry into the realm of optical limiting and optical switching materials for photonic and optoelectronic devices.

Supporting Information Available: Details of synthesis, microscopy, spectroscopy, and nonlinear optical studies and computations. This material is available free of charge via the Internet at http://pubs.acs.org.

performance of the Graphene-C_{60} sample is close to those of both fullerene and CNT samples in the nanosecond regime, whereas the response of the Graphene-C_{60} to picosecond pulses is similar to that of the CNTs but differs from the behavior of fullerene.[23] The similarity between the NLO action of the Graphene-C_{60} and CNTs suggests that nonlinear scattering, which is known to be responsible for limiting action in CNTs,[22] should play an important role in the NLO action of the Graphene-C_{60}. This is in agreement with the experimental results shown in Figure 4. In addition, the picosecond Z-scan measurements of Graphene-TPP were also carried out and a similar phenomenon was observed.

Figure 6 gives the open-aperture Z-scan curves of Graphene-C_{60} (a) and Graphene-TPP (b) with different input fluences. Using the Crank−Nicolson finite-difference scheme, we fitted the Z-scan curves numerically (solid lines) and obtained the values of effective nonlinear absorption coefficient, β, as shown in Figure 6. In general, the value of β will decrease as input fluence increases for RSA process because of the saturation of RSA,[1] but it will be unchanged for two-photon absorption process. However, the increase of β with input fluence implies that besides nonlinear absorption from GO and porphyrin (or fullerene) the observed NLO performance is also influenced by nonlinear scattering in the high-fluence regime for two graphene hybrid materials. The similar phenomena have been observed in the porphyrin covalently functionalized SWNTs.[8] Comparing the values of β between the Graphene nanohybirds and SWNT-TPP system in ref 8, it can be found that Graphene nanohybirds have larger effective nonlinear absorption coefficient, which is up to 478 cm/GW. However, it should be noted that we used higher input fluence and sample concentrations in our experiments compared with those in ref 8.

From the above discussions we can see that besides nonlinear absorption the graphene hybrids covalently functionalized with porphyrin and fullerene have strong nonlinear

References and Notes

(1) Sutherland, R. L. *Handbook of Nonlinear Optics,*2nd ed.; Marcel Dekker: New York, 2003.

(2) Tutt, L. W.; Boggess, T. F. *Prog. Quantum Electron.* **1993**, *17*, 299.

(3) Chen, P.; Wu, X.; Sun, X.; Lin, J.; Ji, W.; Tan, K. L. *Phys. Rev. Lett.* **1999**, *82*, 2548.

(4) Hagan, D. J.; Xia, T.; Said, A. A.; Wei, T. H.; Van Stryland, E. W. *J. Nonlinear Opt. Phys. Mater.* **1993**, *2*, 483.

9686 *J. Phys. Chem. B, Vol. 113, No. 29, 2009*

Liu et al.

(5) Webster, S.; Reyes-Reyes, M.; Pedron, X.; López-Sandoval, R.; Terrones, M.; Carroll, D. L. *Adv. Mater.* **2005**, *17*, 1239.

(6) Mhuircheartaigh, E. M. N.; Giordani, S.; Blau, W. J. *J. Phys. Chem. B* **2006**, *110*, 23136.

(7) Wang, J.; Blau, W. J. *Chem. Phys. Lett.* **2008**, *465*, 265.

(8) Liu, Z. B.; Tian, J. G.; Guo, Z.; Ren, D. M.; Du, F.; Zheng, J. Y.; Chen, Y. S. *Adv. Mater.* **2008**, *20*, 511.

(9) Guo, Z.; Du, F.; Ren, D. M.; Chen, Y. S.; Zheng, J. Y.; Liu, Z. B.; Tian, J. G. *J. Mater. Chem.* **2006**, *16*, 3021.

(10) Senge, M. O.; Fazekas, M.; Notaras, E. G. A.; Blau, W. J.; Zawadzka, M.; Locos, O. B.; Ni Mhuircheartaigh, E. M. *Adv. Mater.* **2007**, *19*, 2737.

(11) McEwan, K.; Fleitz, P.; Rogers, J.; Slagle, J.; McLean, D.; Akdas, H.; Katterle, M.; Blake, I.; Anderson, H. *Adv. Mater.* **2004**, *16*, 1933.

(12) Tutt, L. W.; Kost, A. *Nature* **1992**, *356*, 225.

(13) McLean, D. G.; Sutherland, R. L.; Brant, M. C.; Brandelik, D. M.; Fleitz, P. A.; Pottenger, T. *Opt. Lett.* **1993**, *18*, 858.

(14) Li, D.; Kaner, R. B. *Science* **2008**, *320*, 1170.

(15) Dikin, D. A.; Stankovich, S.; Zimney, E. J.; Piner, R. D.; Dommett, G. H. B.; Evmenenko, G.; Nguyen, S. T.; Ruoff, R. S. *Nature* **2007**, *448*, 457.

(16) Bunch, J. S.; van der Zande, A. M.; Verbridge, S. S.; Frank, I. W.; Tanenbaum, D. M.; Parpia, J. M.; Craighead, H. G.; Mceuen, P. L. *Science* **2007**, *315*, 490.

(17) Liu, Z. B.; Wang, Y.; Zhang, X. L.; Xu, Y. F.; Chen, Y. S.; Tian, J. G. *Appl. Phys. Lett.* **2009**, *94*, 021902.

(18) Xu, Y. F.; Liu, Z. B.; Zhang, X. L.; Wang, Y.; Tian, J. G.; Huang, Y.; Ma, Y. F.; Chen, Y. S. *Adv. Mater.* **2009**, *21*, 1275.

(19) Zhang, X. Y.; Huang, Y.; Wang, Y.; Ma, Y. F.; Liu, Z. F.; Chen, Y. S. *Carbon* **2009**, *47*, 334.

(20) Becerril, H. A.; Mao, J.; Liu, Z. F.; Stoltenberg, R. M.; Bao, Z. N.; Chen, Y. S. *ACS Nano.* **2008**, *2*, 463.

(21) Sheikbahae, M.; Said, A. A.; Wei, T. H.; Hagan, D. J.; Vanstryland, E. W. *IEEE J. Quantum Electron.* **1990**, *26*, 760.

(22) Vivien, L.; Lancon, P.; Riehl, D.; Hache, F.; Anglaret, E. *Carbon* **2002**, *40*, 1789.

(23) Sun, X.; Xiong, Y.; Chen, P.; Lin, J.; Ji, W.; Lim, J. H.; Yang, S. S.; Hagan, D. J.; Van Stryland, E. W. *Appl. Opt.* **2000**, *39*, 1998.

(24) Vivien, L.; Riehl, D.; Delouis, J. F.; Delaire, J. A.; Hache, F.; Anglaret, E. *J. Opt. Soc. Am. B* **2002**, *19*, 208.

(25) Li, H.; Martin, R. B.; Harruff, B. A.; Carino, R. A.; Allard, L.; Sun, Y. P. *Adv. Mater.* **2004**, *16*, 896.

(26) Wu, W.; Zhu, H. R.; Fan, L. Z.; Yang, S. H. *Chem.—Eur. J.* **2008**, *14*, 5981.

(27) Wu, W.; Zhang, S.; Li, Y.; Li, J.; Liu, L.; Qin, Y.; Guo, Z. X.; Dai, L.; Ye, C.; Zhu, D. *Macromolecules* **2003**, *36*, 6286.

Supporting Information for

Porphyrin and Fullerene Covalently Functionalized Graphene Hybrid Materials with Large Nonlinear Optical Properties

Zhi-Bo Liu,[†]   Yan-Fei Xu,[‡]   Xiao-Yan Zhang,[‡] Xiao-Liang Zhang,[†] Yong-Sheng Chen,*,[‡] Jian-Guo Tian*,[†]

[†] *The Key Laboratory of Weak Light Nonlinear Photonics, Ministry of Education, Teda Applied Physics School, Nankai University, Tianjin 300457, P. R. China.*
[‡] *Key Laboratory for Functional Polymer Materials and Centre for Nanoscale Science and Technology, Nankai University, Tianjin 300071, P. R. China.*

Contents

1. **Synthesis**

2. **Instruments and measurements.**

3. **Microscopy and Spectroscopy**

4. **Nonlinear optical studies**

5. **Computations**

1. Synthesis

Synthesis of Graphene-TPP: The synthesis of Graphene-TPP is shown in Scheme 1. TTP-NH$_2$ was synthesized according to the literature.[1] Graphene oxide (30 mg) was prepared using our modified Hummers method.[2] and it was then refluxed in SOCl$_2$ (20 ml) in the presence of DMF (0.5 ml) at 70 ^{o}C for 24 h under argon atmosphere. At the end of the reaction, excess SOCl$_2$ and solvent were removed by distillation. In the presence of triethylamine (Et$_3$N, 0.5 ml), the above product was allowed to react with TTP-NH$_2$ (30 mg) in DMF (10 ml) at 130 ^{o}C for 72 h under argon. After the reaction, the solution was cooled to room temperature, and then poured into aether (300 ml) to precipitate the product. The product was isolated by filtration on a Nylon membrane (0.22 μm). The excess TTP-NH$_2$ and other impurities were removed through 5 washing cycles that included sonication, filtration (discarding the filtrate), re-suspending the solid in THF (50 ml) each time. The precipitate was washed with CHCl$_3$ 5 times following the above procedure. UV and TLC were used to check the filtrate to ensure no TTP-NH$_2$ existed in the final washing. And then Graphene-TPP was washed with a small quantity of H$_2$O to remove Et$_3$N·HCl, and finally dried under vacuum to yield the hybrid Graphene-TPP.

Synthesis of Graphene-C$_{60}$: The synthesis of Graphene-C$_{60}$ is shown in Scheme 2. Pyrrolidine fullerene was prepared by a photochemical reaction between amine acid esters and C60 [3]. GO (50 mg) was reacted with SOCl$_2$ (20 ml) in the presence of N,N-dimethyl-formamide (DMF) (0.5 ml) at 70 ^{o}C for 24 h to abtain the acyl-chloride functionalized GO. The excess SOCl$_2$ was evacuated under reduced pressure, and washed with anhydrous toluene for three times to remove the residual SOCl$_2$. Then pyrrolidine fullerene (44 mg) and triethylamine (1 ml) in CHCl$_3$ (40 ml) were added to the above residue. The solution was purged with Ar and stirred for 3 days in dark at room temperature. On completion of the reaction, the solution was poured into acetone. The resultant suspension was collected on a polycarbonate membrane filter of 100 nm pore size and washed with CHCl$_3$ (sonication) for several times until the unreacted pyrrolidine fullerene was completely removed (monitored by thin layer

chromatography). The deposition was further washed with water and acetone, then dried under vacuum to yield Graphene-C_{60} hybrid (24 mg).

2. Instruments and measurements.

FTIR spectra were obtained with a BRUKER TENSOR 27 instrument. All IR samples were prepared as pellets using spectroscopic grade KBr. UV-Vis spectra were obtained with a JASCO V-570, and UV-Vis spectra were recorded on a VARIAN Cary 300 spectrophotometer using a quartz cell with a path length of 10 mm. Raman spectra were measured by a Renishaw inVia Raman microscope at room temperature with the 514 nm line of an Ar ion laser as an excitation source. Fluorescence spectra were obtained with a FluoroMax-P instrument. Transmission electron microscope (TEM) images were obtained on a JEM.2010FEF instrument operated at 200 kV. Sample preparation involved water bath sonicating (Gongyi Yuhua Instrument Co., LTD, Model: KQ400B, 400 W) materials in DMF for 2h and dropping the resulting suspension onto carbon-coated copper grids. H^1NMR spectra were recorded on a BRUKER (300 MHz) spectrometer using TMS as the internal standard. Tapping mode AFM measurements were performed using Multimode SPM from Digital Instruments with Nanoscope IIIa Controller and the samples for AFM images were prepared by depositing a dispersion of graphene oxide/H_2O solution (0.2 mg/ml) on a freshly cleaved mica surface. Graphite was obtained from Qingdao Huarun graphite Co. Column chromatography was performed with silica gel (100-200 mesh, Qingdao Haiyang Chemical Co., Ltd, China).

3. Microscopy and Spectroscopy.
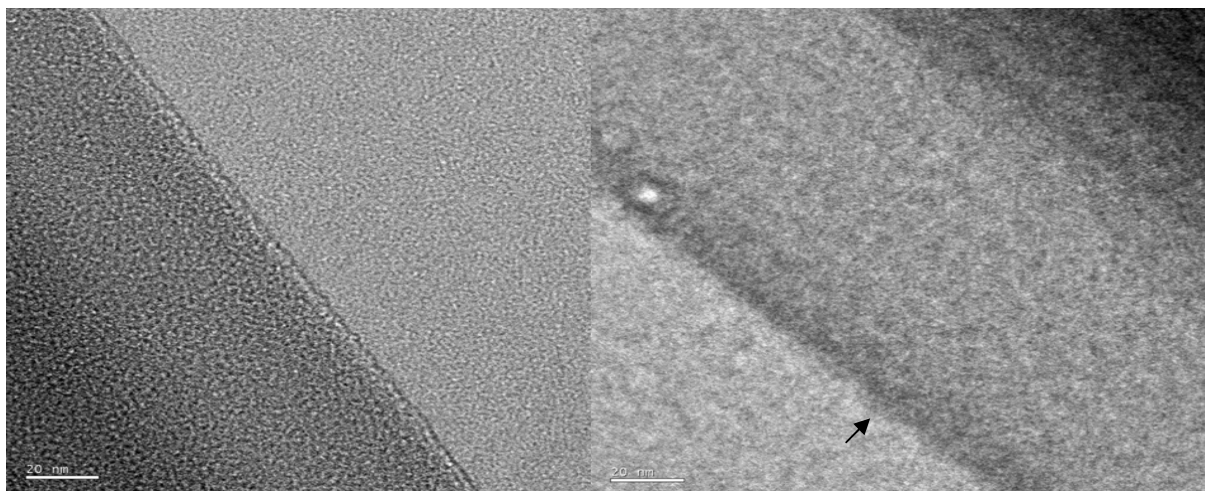
Fig. S1. TEM images of graphene oxide (left) and Graphene-TPP (right). The edge of graphene oxide was significantly roughened by the coverage of soft material, indicating the presence of TTP-NH$_2$ attached to the graphene oxide edge.
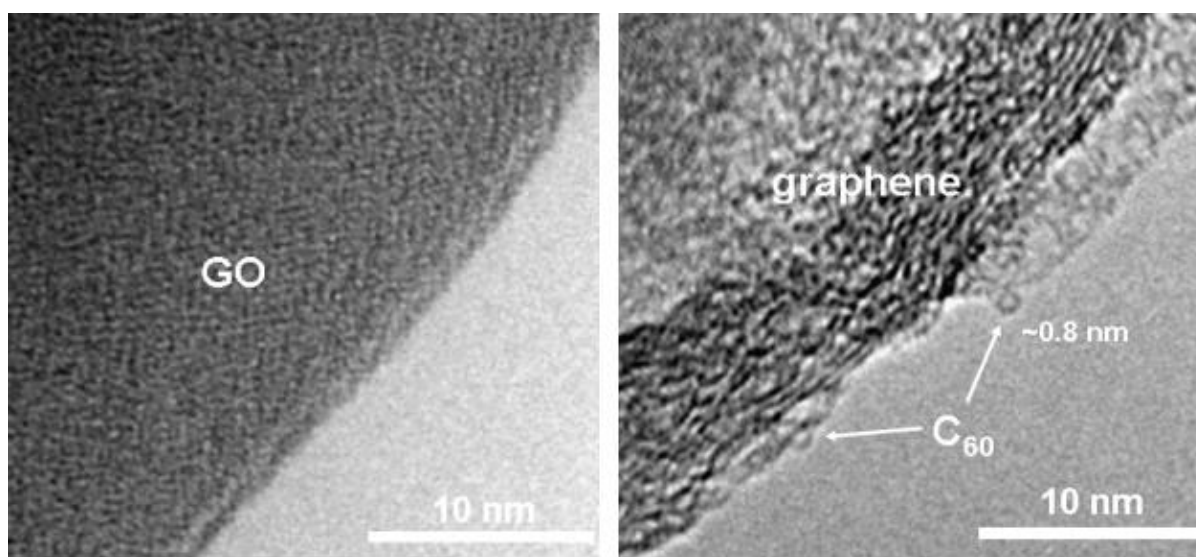
Fig. S2. TEM images of GO (left) and graphene–C60 hybrid (right). The images were acquired from samples deposited onto a holey carbon support film.
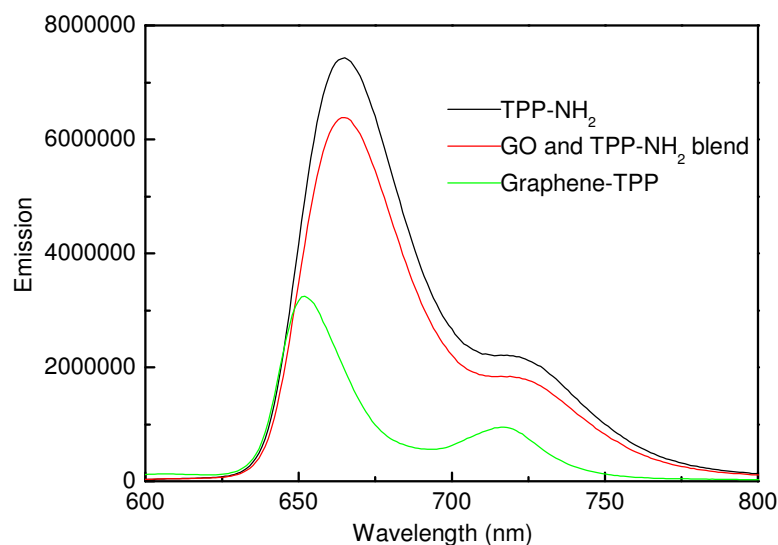
Fig. S3. Fluorescence spectral changes observed for TPP-NH$_2$, the controlled sample, Graphene-TPP in DMF with the normalization of the absorbance of the Soret band excitation wavelength (419 nm) to the same value (0.24). The observed luminescence quenching indicated that there was a strong interaction between the excited state of TPP and graphene moieties in the hybrid.
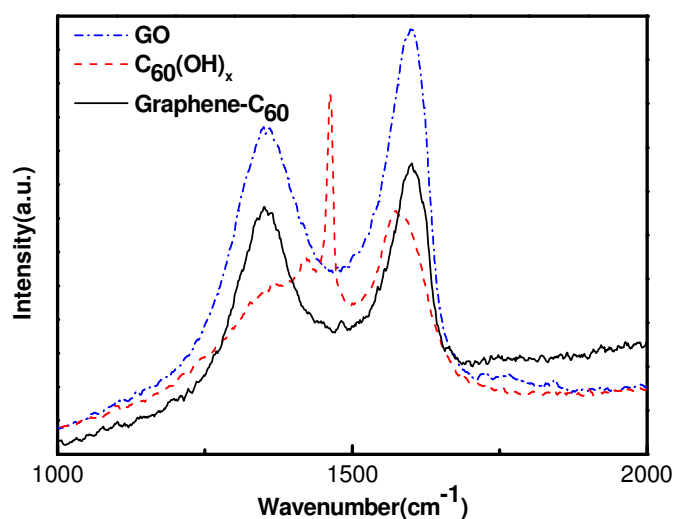

Fig. S4. Raman spectra of GO (dashed line), pyrrolidine fullerene (dotted line) and Graphene–C$_{60}$ (solid line) excited at 514 nm. The peak at 1482 cm^{-1} in the Graphene–C$_{60}$ is the Ag(2) mode of the C$_{60}$ cage, which is shifted by 13 cm^{-1} compared with that of the pyrrolidine–C$_{60}$. This relative shift sufficiently suggests a strong interaction between the C$_{60}$ cage and the graphene sheet.

4. Nonlinear optical studies.
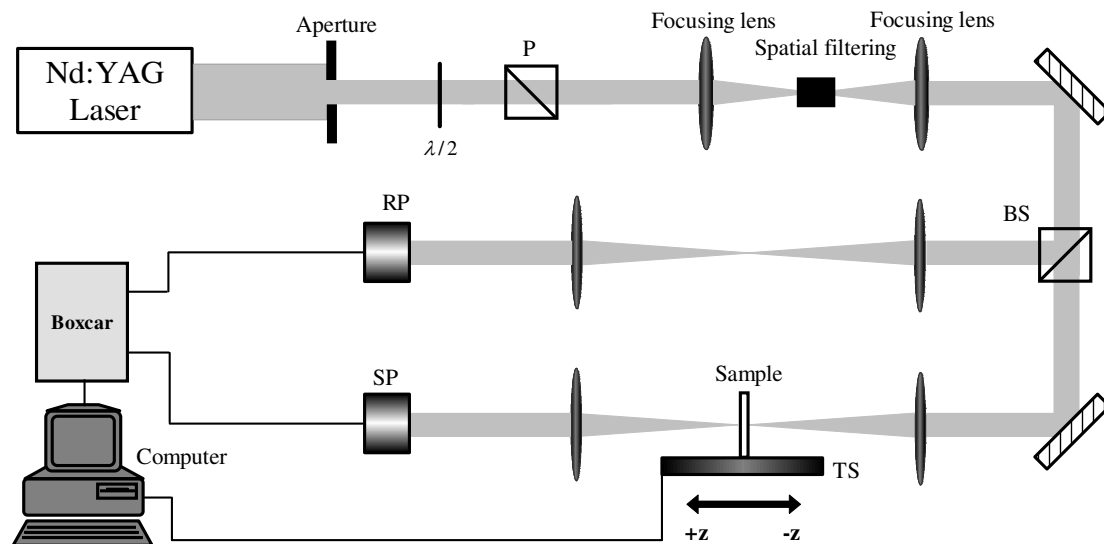
Fig. S5. Setup of Z-scan experiments. P = polarizer, BS = beam splitter, RP = reference detector, SP = signal detector.
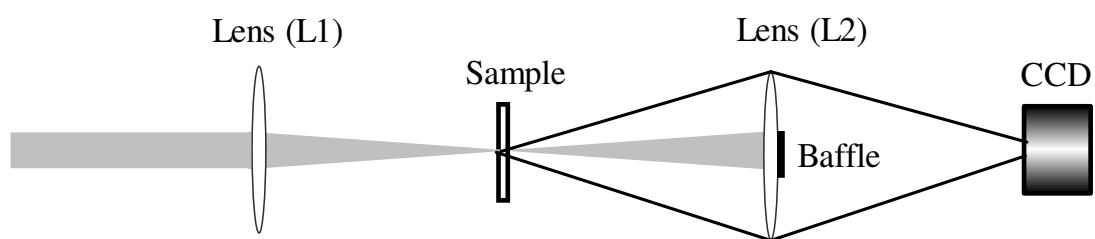
Fig. S6. Setup of the nonlinear scattering experiments.

5. Computations.

To compare quantitatively, we theoretically fitted the experimental results of open aperture Z-scan to obtain effective nonlinear absorption coefficients β.[4] Because the length L of the samples used in our experiments was longer than the Rayleigh length of beam z_0, a thick sample model and a numerical method were used to solve the propagation equation of the electric field envelope. The partial differential equation that describes the propagation of the electric field envelope E in a nonlinear medium can be written as:

$$\frac{1}{r}\frac{\partial}{\partial r}\left(r\frac{\partial E}{\partial r}\right) - 2ik\frac{\partial E}{\partial z} - ik\alpha E + \frac{2k^2}{n_0}n_2|E|^2 \cdot E = 0 , \tag{1}$$

$$\alpha = \alpha_0 + \beta \cdot I , \tag{2}$$

where α_0 is linear absorption coefficient, n_2 is nonlinear refractive index, and k is wave vector. The numerical simulation of Eq. (1) was made by the Crank–Nicholson finite difference method.

Reference:

[1] W. J. Kruper, T. A. Chamberlin, M. Kochanny, J. Org. Chem. **1989**, 54, 2753.

[2] H. A. Becerril, J. Mao, Z. F. Liu, R. M. Stoltenberg, Z. N. Bao, Y. S. Chen, Acs Nano. **2008**, 2, 463.

[3] Gan LB, Zhou DJ, Luo CP, Tan HS, Huang CH, Lu MJ, et al. J Org Chem 1996;61(6):1954–61.

[4] E. M. N. Mhuircheartaigh, S. Giordani, W. J. Blau, J. Phys. Chem. B **2006**, 110, 23136.